Journal of Zhejiang University SCIENCE A
ISSN 1673-565X (Print); ISSN 1862-1775 (Online)
www.zju.edu.cn/jzus; www.springerlink.com
E-mail: jzus@zju.edu.cn

High-finesse displacement sensor and a theoretical accelerometer model based on a fiber Fabry-Perot interferometer*

Xu ZENG†, Yu WU, Chang-lun HOU, Guo-guang YANG

(*State Key Laboratory of Modern Optical Instrumentation, Zhejiang University, Hangzhou 310027, China*)

†E-mail: zengxu@zju.edu.cn

Received Apr. 9, 2008; Revision accepted July 17, 2008; Crosschecked Feb. 9, 2009

Abstract: A displacement sensor based on the fiber Fabry-Perot (F-P) cavity was proposed in this paper. Theoretical and experimental analyses were presented. Displacement resolution was demonstrated by spectrum-domain experiments to obtain the dynamic range of the F-P sensor, and a piezoelectric crystal unit (PZT) was used as the driver. The output signal was modulated by a piezoelectric ceramic ring and demodulated by a phase-locked oscillator. The experimental results show that the displacement resolution of the F-P sensor is less than 5 nm and the dynamic range is more than 100 μm. As acceleration is the second-order differential of displacement, an accelerometer model was proposed using the finite element method (FEM) nd ANSYS software.

Key words: Fiber Fabry-Perot (F-P) sensor, Spectrum demodulation, Micro-displacement measurement, Accelerometer model
doi:10.1631/jzus.A0820270 **Document code:** A **CLC number:** O43

INTRODUCTION

Nano- and micro-scale displacement sensors have been widely used in various fields, including micro-manipulating, micro-manufacture, precisely positioning, and so on. Several kinds of displacement sensors have been proposed in the literature, such as the capacitive displacement sensor (Genossar and Steinitz, 1990; Roth and Gmelin, 1992), the piezoelectric displacement sensor (Akamine *et al.*, 1989), and the optical lever displacement sensor (Meyer and Amer, 1988). Of these techniques, a displacement sensor based on fiber optics holds the best promise for high precision, for measuring in hostile environments, and for its immunity to electromagnetic interference.

In this paper, a displacement sensor based on the principle of the fiber Fabry-Perot (F-P) interferometric sensor is presented. Compared with existing fiber-optics-based displacement sensors (Rugar *et al.*, 1988; Zheng and Albin, 1998; Niu *et al.*, 2005), the F-P sensor has the advantages of high sensitivity, small size, easy implementation, and low cost. On the other hand, microelectromechanical system (MEMS) technology is rapidly spreading internationally. MEMS technology has advantages over traditional mechanical technology, especially on account of high sensitivity and compact size. Therefore, the approach of combining MEMS technology with the interferometer measurement technique may result in a development in microsensors. Based on this idea, we propose a novel micro-accelerometer model consisting of a fiber F-P interferometric sensor and MEMS mass.

In Section 2 of this paper, the basic structure of a fiber F-P sensor and the experiment system are introduced. In Section 3, the demodulation method in the spectrum domain is proposed. As acceleration is the second-order differential of displacement, by the use of the finite element method (FEM), a structure for the accelerometer is proposed theoretically in Section 4. In Section 5, the experimental results and error analysis are presented in both the spectrum domain and the time domain. Finally Section 6 concludes the paper.

* Project (No. 111303-8112D2) supported by the National Defense Research Foundation of Zhejiang University, China

BASIC STRUCTURE

As shown in Fig.1, a typical fiber F-P sensor consists of a hollow-core tube and two fibers to form a high-finesse cavity. Each end of the fiber is coated with a high reflective membrane. When the fiber is used for sensing, one of the fibers is fixed, and the other one is movable. The movable fiber is fixed on the mass, and the fixed one is bonded to the plastic hollow-core tube, which is used to protect the fiber from environmental damage. The gap between the two reflectors is used as the sensing part. Light launched into the cavity will lead to multi-beam interference. Hence, the cavity length, or sensor gap, can be accurately measured to the precision of a few nanometers using a straightforward white light readout system. To avoid external vibration, the 3D translation stage, which is used as the foundation of a piezoelectric crystal unit (PZT), is fixed on an optical platform to isolate the radial vibration.

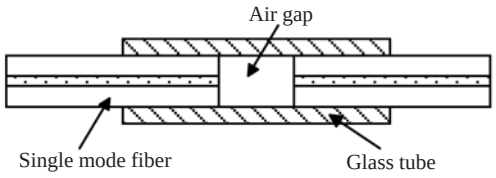

Fig.1 Basic structure of an F-P sensor

The experimental arrangement for analyzing the F-P displacement sensor is illustrated in Fig.2. In this study, two testing methods, one measuring the light intensity in the time domain, and the other measuring the spectrum in the frequency domain, are introduced. The supported photo-electronics is composed of a laser diode, a PZT ceramics, a testing instrument, and a 2×2 fused biconical tapered coupler. The transmission fiber is a standard single-mode optical fiber (the Corning® single-mode fiber, SMF-28). In the frequency domain measuring experiment, a broadband laser diode with center wavelength at 840 nm and width 50 nm was adopted. The light was injected into the F-P sensor and received by a fiber spectrometer through two fiber connection/physical contact (FC/PC) connectors.

The laser light is guided into an isolator, which eliminates the feedback from the fiber into the laser, before the fiber pigtail is connected with a 2×2 directional coupler. The 2×2 directional coupler is used as a beam splitter in our experiment. A portion of light, about 50% of the input optical power, passes through the 2×2 coupler to the fiber F-P sensor, and then reflects back to the detector. In order to detect the dynamical change of the F-P cavity, another PZT was used as the driver. The moveable part of the F-P sensor was bonded with the PZT.

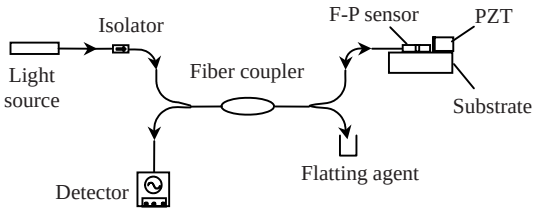

Fig.2 Schematic of experimental arrangement used to detect the time and spectrum domain signals from an F-P sensor

THEORETICAL MODEL

In order to deduce the relationship between the output signal and the length of F-P cavity in the frequency domain, a spectrum interpolation method was adopted (Zhang *et al.*, 2005). We assume that the incident light is in the form of a Gauss beam, given as follows:

$$I_0(\lambda) = I_0 \exp[(\lambda - \lambda_p)^2 / B_\lambda^2], \qquad (1)$$

where I_0 is the normalized intensity of the incident light, λ_p is the peak wavelength, and B_λ is the spectral bandwidth.

When light is launched into the movable fiber of the F-P sensor, most of the power is transmitted to the fixed one. However, part of the light is reflected by the end face of the fixed fiber. The reflected light is repeatedly reflected by the first fiber. The phase difference of these two light paths causes multi-interference in the optical receiver. According to the principle of multi-beam interference, the distribution of light emitted from the fiber can be given as

$$I_r = \frac{2R[1-\cos(4\pi l/\lambda)]}{1+R^2-2R\cos(4\pi l/\lambda)} I_0(\lambda), \qquad (2)$$

where R is the reflectivity of the reflectors, l is the cavity length. Although the transmission losses at 840 nm will affect the light intensity, actually in the

frequency domain testing, the cavity length just depends on the spectrum distribution and can be detected by the spectrometer. The denominator of the right hand side of Eq.(2) can be approximately 1 when $R\to 0$, and by substituting the wavelength λ with c/ν, where c is the light velocity and ν is the light frequency, Eq.(2) can be expressed as

$$I_r = 2R[1-\cos(4\pi l\nu / c)]I_0(\lambda). \tag{3}$$

Substituting Eq.(1) into Eq.(3), and replacing the wavelength λ with c/ν, the output light can be given as follows:

$$I_r = 2R[1-\cos(4\pi l\nu / c)]I_0 \exp\left[-\frac{(\nu-\nu_p)^2}{2(\sigma_\lambda \nu\nu_p / c)^2}\right], \tag{4}$$

where $\nu_p=c/\lambda_p$, $\sigma_\lambda = B_\lambda / \sqrt{2}$. Using Taylor series expansion, the exponent part of Eq.(4) can be expressed as

$$\frac{\nu-\nu_p}{\nu}=\frac{\nu-\nu_p}{\nu_p}-\frac{(\nu-\nu_p)^2}{\nu_p^2}+\cdots=\frac{\nu-\nu_p}{\nu_p}\left(1-\frac{\nu-\nu_p}{\nu_p}+\cdots\right). \tag{5}$$

Taking the first-order approximation of Eq.(5) and substituting it into Eq.(4), we obtain the output light in the frequency domain as

$$I(\nu)\approx 2R[1-\cos(4\pi l\nu / c)]I_0 \exp\left[-\frac{(\nu-\nu_p)^2}{2\sigma_\nu^2}\right]. \tag{6}$$

In order to demodulate the cavity length of the F-P sensor, Eq.(6) was processed by using the fast Fourier transform, and the result can be obtained as follows:

$$\begin{aligned}F(\mathrm{j}\xi) &= 2\sqrt{2\pi}RI_0\sigma_\nu\left[\exp(-\mathrm{j}\nu_p\xi)\exp\left(-\frac{\sigma_p^2\xi^2}{2}\right)\right]\\ &+\sqrt{2\pi}RI_0\sigma_\nu\left\{\exp\left[-\mathrm{j}\left(\xi-\frac{4\pi l}{c}\right)\nu_p\right]\exp\left[-\frac{\sigma_\nu^2}{2}\left(\xi-\frac{4\pi l}{c}\right)^2\right]\right\}\\ &+\sqrt{2\pi}RI_0\sigma_\nu\left\{\exp\left[-\mathrm{j}\left(\xi+\frac{4\pi l}{c}\right)\nu_p\right]\exp\left[-\frac{\sigma_\nu^2}{2}\left(\xi+\frac{4\pi l}{c}\right)^2\right]\right\}.\end{aligned} \tag{7}$$

From Eq.(7), it can be observed that there exist two extreme points—one contains the intensity information and the other, which can be expressed as $\xi_l=4\pi l/c$, contains the details of the F-P cavity length l.

The data sampled by the spectrometer varied with wavelength; however, the demodulating method above is based on the frequency domain. Therefore the sampling data should be converted to the frequency domain. Assume that the wavelength of the light source ranges from λ_{min} to λ_{max}, and that the number of sampling points in a cycle is N, and then the wavelength interval can be expressed as

$$\delta\lambda = (\lambda_{max}-\lambda_{min})/N, \tag{8}$$

which corresponds to the frequency as

$$\delta\nu = \frac{c}{\lambda}-\frac{c}{\lambda+\delta\lambda}=\frac{c\cdot\delta\lambda}{\lambda(\lambda+\delta\lambda)}. \tag{9}$$

Due to the Gauss distribution of the light source, most of the light intensity is concentrated in the center wavelength. As a result, Eq.(9) can be equivalent to

$$\delta\nu = c\cdot\delta\lambda / \lambda_p^2. \tag{10}$$

After changing the data in the frequency domain and using the fast Fourier transform,

$$X(k)=\sum_{n=0}^{N-1}x(n)\exp(-\mathrm{j}2\pi nk / N). \tag{11}$$

The cavity length can be demodulated by searching the extreme point of $X(k)$. According to the relationship between angular frequency ξ_l and numerical frequency ω_l below:

$$\xi_l = 4\pi l / c,\ \ \omega_l = 2\pi k_l / N,\ \ \omega_l = \xi_l\cdot\delta\nu, \tag{12}$$

where k_l is the abscissa of the extreme point, the cavity length can be deduced as

$$l=\frac{ck_l}{2N\cdot\delta\nu}. \tag{13}$$

Base on Eq.(13), we can deduce the cavity length from spectrum data.

In the time domain testing, the output intensity of the F-P sensor attenuates with the increase in cavity length. The output optical intensity can be given as (Lv *et al.*, 2007)

$$I_r = \frac{RI_0[1+\alpha_l^2-2\alpha_l\cos(4\pi nL/\lambda)]}{1+(R\alpha_l)^2-2(R\alpha_l)\cos(4\pi nL/\lambda)}, \quad (14)$$

where α_l is the loss in the cavity.

ACCELEROMETER MODEL

As displacement is the quadratic differential of acceleration, by use of the FEM, a kind of mass, which transfers the displacement to the acceleration by a special elastic beam, can be created. FEM software ANSYS 10.0 is used for simulation. As shown in Fig.3, the structure of the accelerometer consists of a mass, a beam, and the periphery structure. As a result of the development of MEMS technology, the mass can be fabricated through microlithography, micromachining, or microfabrication.

Fig.3a shows the system structure simulated by ANSYS 10.0. The dimension of the mass is 6 mm×4 mm×0.3 mm, the dimension of the stress cantilever is 2.2 mm×0.3 mm×5 μm, and the dimension of the transition-folding beam is 0.5 mm×0.3 mm×50 μm. The accelerometer is made of silicon. During the simulation we selected the element type 'solid 92' in ANSYS 10.0 and meshed the model with the free shape.

The simulation results show that the resonant frequencies for the first, second, and third simulations along the *X*-axis are 254.76 Hz (Fig.3b), 601.72 Hz (Fig.3c), and 811.78 Hz (Fig.3d), respectively. From the results we can see that below the frequency of 1 kHz, the linearity of the system is acceptable. Based on the results of FEM simulation, the impulse response displacement varies from 0.32 nm to 1.6 mm, which linearly corresponds to the acceleration range of $10^{-5}g$~$50g$. Therefore, according to the displacement resolution of the F-P sensor, we can obtain the acceleration resolution.

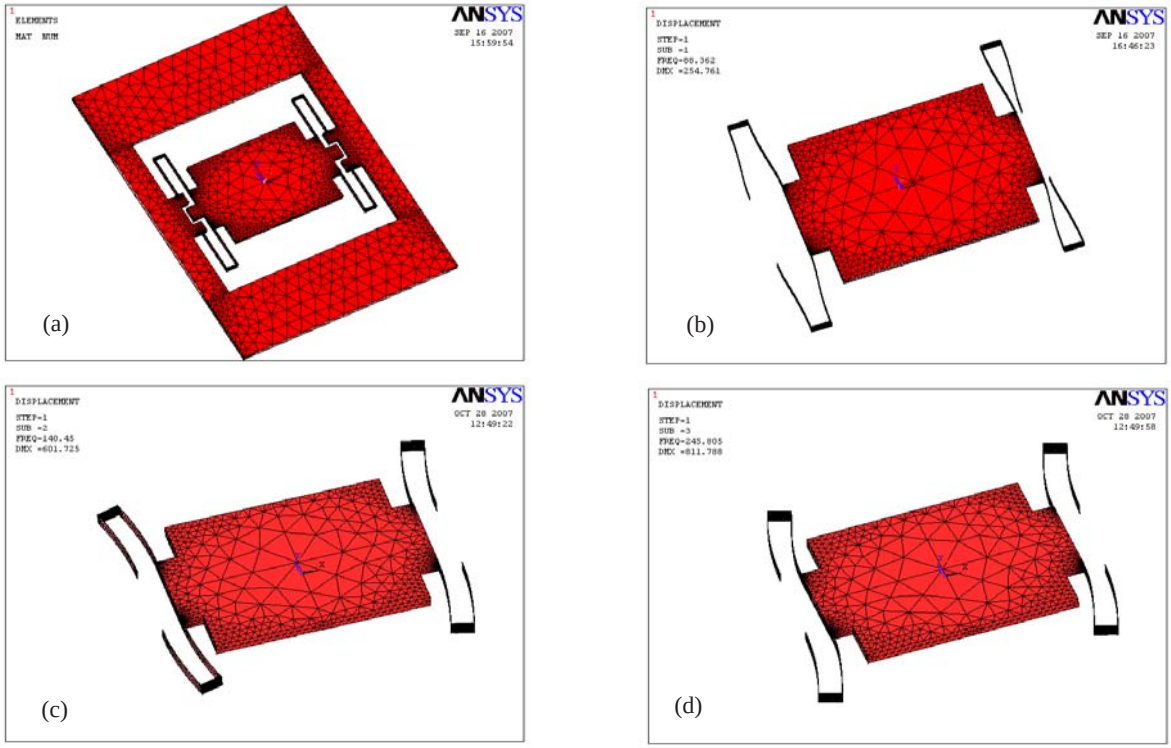

Fig.3 Simulation by ANSYS 10.0 of the accelerometer using the finite element method

(a) System structure; (b) Mode A, resonant frequency 254.76 Hz; (c) Mode B, resonant frequency 601.72 Hz; (d) Mode C, resonant frequency 811.78 Hz

The basic structure of the F-P accelerometer is shown in Fig.4. First of all, the plastic tube of the F-P sensor is adhered to the periphery of the structure by adhesives. After that, through an accuracy alignment method, the other end is fixed on the mass and inserted in the tube. The diagram shows a compact discharging device structure.

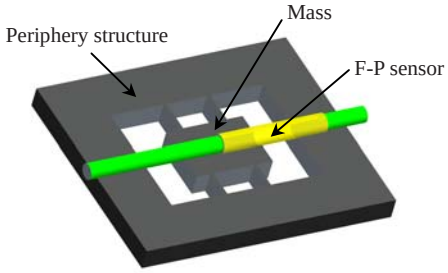

Fig.4 Monolithic construction of a MEMS fiber F-P accelerometer

EXPERIMENTAL VERIFICATION

To verify the above models, the output signals were experimentally obtained according to the change in the air gap, using a 3D translator and a PZT. Both the frequency- and time-domain signals were detected by a spectrometer and an oscilloscope.

Fig.5 shows the trend between the optical spectrum and the F-P cavity length. When the cavity length increases, the optical spectrum has a higher density. The diagram shows the output spectrum as the cavity length is 7.35, 10.41, 18.75, 27.35, or 33.87 μm. The light intensity decreases with the increase of the F-P gap, which is caused by the multiple reflection dissipation.

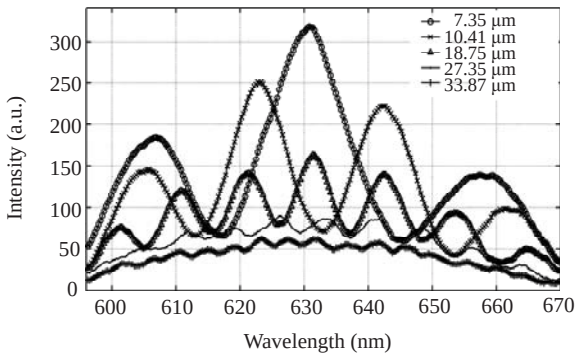

Fig.5 Output spectrum of the F-P sensor when the cavity length is 7.35, 10.41, 18.75, 27.35, or 33.87 μm

Based on Eq.(3), the cavity length can be demodulated by the discrete Fourier transform. The experiment values accord with the theoretical values, as shown in Fig.6. The cross correlation coefficient is 0.9958. As the minimum step size of the PZT is 5 nm and this change can also be demodulated by the Fourier transform, the minimum resolution of the F-P sensor is less than 5 nm.

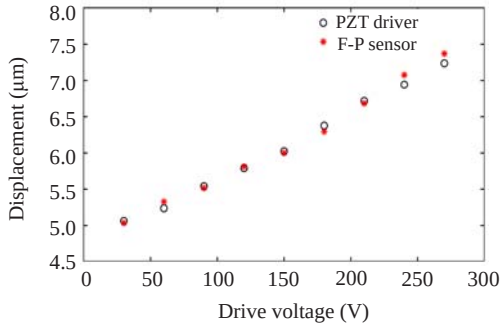

Fig.6 Displacement measured by an F-P cavity and a PZT driver

In the intensity test experiment, according to the fiber type, the light source used in this experiment was a single-mode He-Ne laser of 632.8-nm wavelength and 2-nm spectral width. The light was coupled into the F-P sensor using a self-focusing lens. The output light was received by a photodiode and analyzed by an oscilloscope. In order to improve the signal-to- noise ratio, a PZT was used in the input channel of the coupler. The light source was modulated by the PZT and demodulated by a phase-locked oscillator.

Fig.7 shows the output signal in time domain. On the upward side of Fig.7 is the modulated signal, and below the modulated signal is the demodulated signal, showing that the signal can be precisely demodulated by high-frequency modulation. In order to verify the dynamic range of the F-P sensor, another large-range PZT was adopted. The output displacement of the PZT was measured by a capacitance micrometer, and the maximum output displacement is 100 μm. Fig.8 shows the characteristic curve of the PZT.

Fig.9 shows the variation of optical intensity when the PZT drive voltage varies from 0 to 120 V. The initial cavity length is about 5 μm. As the maximum output dynamic range of the PZT is 100 μm, at this time the optical signal can still coincide with the driver's. So we can conclude that the dynamic range of the F-P sensor is more than 100 μm.

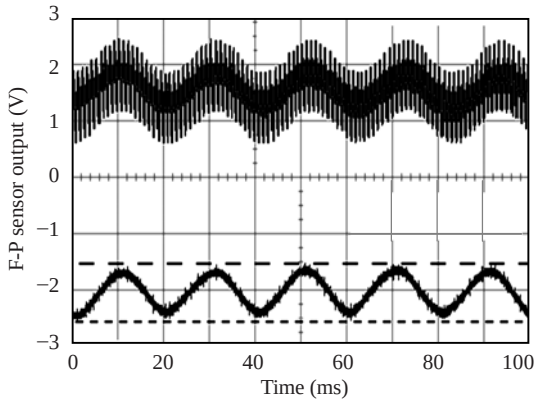

Fig.7 Dynamic range measured by an oscilloscope
The input signal is modulated by a PZT (above), and the output signal is demodulated by a lock-in (below)

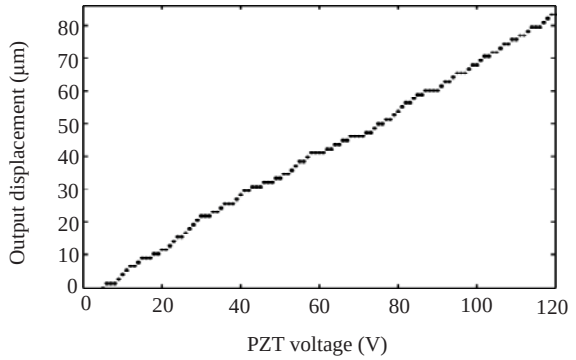

Fig.8 Characteristic curve between PZT voltage and output displacement

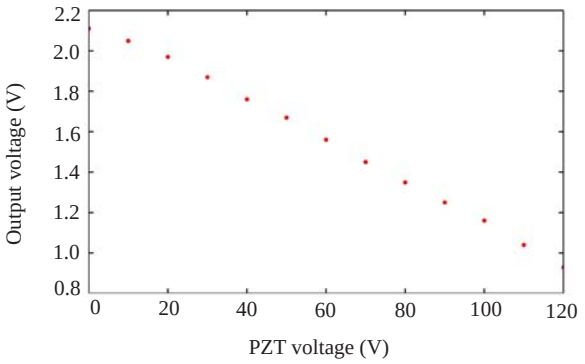

Fig.9 Relationship between output light power and PZT drive voltage

CONCLUSION

In this paper, a high-precision optical nanometer displacement sensor is proposed. Theoretical and experimental analyses are investigated. The experiment measurement consists of two methods. One is based on the spectrum domain test, and the other is based on the time domain test. The minimum displacement resolution is less than 5 nm and the maximum dynamic range of the system is more than 100 μm. Lastly a kind of accelerometer is proposed theoretically. Based on the accelerometer model, a micro-optical accelerometer can be designed combined with MEMS technology.

References

Akamine, S., Albrecht, T.R., Zdeblich, M.J., Quate, C.F., 1989. Microfabricated scanning tunneling microscope. *IEEE Electron Dev. Lett.*, **10**(11):490-492. [doi:10.1109/55.43113]

Genossar, J., Steinitz, M., 1990. A tilted-plate capacitance displacement sensor. *Rev. Sci. Instrum.*, **61**(9):2469-2471. [doi:10.1063/1.1141342]

Lv, T., Du, Q.J., Bi, J., Xiang, D., 2007. Effect of cavity length loss on fiber-optic sensor based on extrinsic Fabry-Perot cavity. *Opto-Electron. Eng.*, **34**(2):130-133 (in Chinese).

Meyer, G., Amer, N.M., 1988. Novel optical approach to atomic force microscopy. *Appl. Phys. Lett.*, **53**(12):1045-1047. [doi:10.1063/1.100061]

Niu, W.C., Yang, Y.F., Kai, G.Y., Dong, X.Y., 2005. Exactitude displacement measurement based on fiber Bragg grating sensors. *Nanotech. Prec. Eng.*, **3**(1):53-55 (in Chinese).

Roth, P., Gmelin, E., 1992. A capacitance displacement sensor with elastic diaphragm. *Rev. Sci. Instrum.*, **63**(3):2051-2053. [doi:10.1063/1.1143165]

Rugar, D., Mamin, H.J., Erlandson, R., Stern, J.E., Terris, B.D., 1988. Force microscope using a fiber-optic displacement sensor. *Rev. Sci. Instrum.*, **59**(11):2337-2340. [doi:10.1063/1.1139958]

Zhang, P., Zhu, Y., Tang, X.C., Chen, W.M., 2005. Demodulation of the optical fiber Fabry-Perot sensor based on Fourier transform. *Acta Opt. Sin.*, **25**(2):186-189 (in Chinese).

Zheng, J., Albin, S., 1998. Self-referenced reflective intensity fiber optic displacement sensor. *Opt. Eng.*, **38**(2):227-232. [doi:10.1117/1.602260]